Metabolic Engineering 25 (2014) 92–102

Contents lists available at ScienceDirect

Metabolic Engineering

journal homepage: www.elsevier.com/locate/ymben

The impact of anti-apoptotic gene Bcl-2Δ expression on CHO central metabolism

Neil Templeton [a], Abasha Lewis [b], Haimanti Dorai [c], Elaine A. Qian [a], Marguerite P. Campbell [c], Kevin D. Smith [c], Steven E. Lang [c], Michael J. Betenbaugh [b], Jamey D. Young [a,d,*]

[a] Department of Chemical and Biomolecular Engineering, Vanderbilt University; PMB 351604, 2301 Vanderbilt Place, Nashville, TN 37235-1604, USA
[b] Department of Chemical and Biomolecular Engineering, Johns Hopkins University; 3400 North Charles Street, Baltimore, MD 21218, USA
[c] Janssen Pharmaceutical J&J, Biologics Research, Biotechnology CoE; 1400 McKean Road, Spring House, PA, 19002 USA
[d] Department of Molecular Physiology and Biophysics, Vanderbilt University; PMB 351604, 2301 Vanderbilt Place, Nashville, TN 37235-1604, USA

ARTICLE INFO

Article history:
Received 13 January 2014
Received in revised form
24 June 2014
Accepted 27 June 2014
Available online 8 July 2014

Keywords:
Apoptosis
Central metabolism
Mitochondria
Lactate
Metabolic flux analysis (MFA)
Chinese hamster ovary (CHO)
Bcl-2

ABSTRACT

Anti-apoptosis engineering is an established technique to prolong the viability of mammalian cell cultures used for industrial production of recombinant proteins. However, the effect of overexpressing anti-apoptotic proteins on central carbon metabolism has not been systematically studied. We transfected CHO-S cells to express Bcl-2Δ, an engineered anti-apoptotic gene, and selected clones that differed in their Bcl-2Δ expression and caspase activity. ^{13}C metabolic flux analysis (MFA) was then applied to elucidate the metabolic alterations induced by Bcl-2Δ. Expression of Bcl-2Δ reduced lactate accumulation by redirecting the fate of intracellular pyruvate toward mitochondrial oxidation during the lactate-producing phase, and it significantly increased lactate re-uptake during the lactate-consuming phase. This flux redistribution was associated with significant increases in biomass yield, peak viable cell density (VCD), and integrated VCD. Additionally, Bcl-2Δ expression was associated with significant increases in isocitrate dehydrogenase and NADH oxidase activities, both rate-controlling mitochondrial enzymes. This is the first comprehensive ^{13}C MFA study to demonstrate that expression of anti-apoptotic genes has a significant impact on intracellular metabolic fluxes, especially in controlling the fate of pyruvate carbon, which has important biotechnology applications for reducing lactate accumulation and enhancing productivity in mammalian cell cultures.

1. Introduction

Chinese hamster ovary (CHO) cells have emerged as the most widely used mammalian cell line for recombinant protein production, accounting for nearly 70% of all biotherapeutics produced in what is approaching a $100 billion global marketplace (Ahn and Antoniewicz, 2012; Aggarwal, 2012). This biologics market is growing at a rate 60% faster than the overall pharmaceutical market (Aggarwal, 2012). Some of the major advantages of CHO cells are their ability to secrete correctly folded and post-translationally modified recombinant proteins and their proven history of regulatory approval (Xu et al., 2011). Increasing demand for biopharmaceutical products requires CHO hosts and culture systems to become more productive, as the costs associated with producing sufficient antibody to conduct clinical trials can account for a substantial portion of the total drug development cost (Zhang, 2010; Farid, 2007). Failure of the scientific community to develop rational approaches for increasing product titer and yield will result in high development costs that stymie both drug discovery and drug affordability.

Manipulating apoptotic pathways is one route that has been used to improve recombinant protein titers. After all, volumetric protein productivity is directly proportional to the integrated viable cell density (IVCD) of the culture (Altamirano et al., 2004), and apoptosis accounts for up to 80% of cell death in a typical bioreactor run (Goswami et al., 1999). Overexpressing anti-apoptotic genes, such as Bcl-2 or Bcl-xL, to limit the progression of apoptosis was shown to be effective at maintaining cell viability in response to a variety of adverse bioreactor conditions (Mastrangelo et al., 1999, 2000; Chiang and Sisk, 2005; Simpson et al., 1998; Fussenegger et al., 2000). More recently, CHO cells overexpressing anti-apoptotic genes E1B-19K, Aven, and an XIAP mutant (XIAPΔ) provided a 60% increase in IVCD and 80% increase in final product titer (Dorai et al., 2009). Interestingly, the apoptosis-resistant clones were also found to accumulate less

* Corresponding author at: Department of Chemical and Biomolecular Engineering, Vanderbilt University; PMB 351604, 2301 Vanderbilt Place, Nashville, TN, 37235-1604, USA.
E-mail address: j.d.young@vanderbilt.edu (J.D. Young).

http://dx.doi.org/10.1016/j.ymben.2014.06.010
1096-7176/

Nomenclature

3PG	3-phosphoglycerate
AcCoA	acetyl-CoA
ACL	ATP citrate lyase
aKG	α-ketoglutarate
Ala.e	alanine.extracellular
AMBIC	ammonium bicarbonate
ANT	adenine nucleotide translocator
Asn.e	asparagine.extracellular
ATP	adenosine-5'-triphosphate
Bcl-2	B-cell lymphoma 2
CHO	Chinese hamster ovary
Cit	citrate
DHAP	dihydroxyacetone phosphate
E4P	erythrose-4-phosphate
EMU	elementary metabolite unit
F6P	fructose 6-phosphate
Fum	fumarate
G6P	glucose-6-phosphate
G6PDH	glucose-6-phosphate dehydrogenase
GAP	glyceraldehyde-3-phosphate
GCMS	gas chromatography–mass spectrometry
Glc	glucose
Gln.e	glutamine.extracellular
HE	high expressing (of Bcl-2Δ)
HPLC	high performance liquid chromatography
HRP	horseradish peroxidase
IDH	isocitrate dehydrogenase
IVCD	integrated viable cell density
Lac.e	lactate.extracellular
Lac	lactate
LDH	lactate dehydrogenase
LE	low expressing (of Bcl-2Δ)
Leu.e	leucine.extracellular
Lys.e	lysine.extracellular
Mal	malate
ME	malic enzyme
MFA	metabolic flux analysis
MID	mass isotopomer distribution
MOX	methoxyamine
MTBSTFA	N-methyl-N-(t-butyldimethylsilyl) trifluoroacetamide
NADH	nicotinamide adenine dinucleotide
NADPH	nicotinamide adenine dinucleotide phosphate
OAA	oxaloacetate
OPA	orthophthaldildehyde
OXPHOS	oxidative phosphorylation
oxPPP	oxidative pentose phosphate pathway
PC	pyruvate carboxylase
PDH	pyruvate dehydrogenase
PEP	phosphoenolpyruvate
PPP	pentose phosphate pathway
Pro	proline
PTP	permeability transition pore
Pyr	pyruvate
R5P	ribose-5-phosphate
RCF	relative centrifugation force
ROS	reactive oxygen species
Ru5P	ribulose-5-phosphate
S7P	sedoheptulose-7-phosphate
Ser.e	serine.extracellular
Suc	succinate
TBDMCS	tert-butyldimethylchlorosilane
TCA Cycle	tri-carboxylic acid cycle
Val.e	valine.extracellular
VCD	viable cell density
VDAC	voltage dependent anion channel
X5P	xylulose-5-phosphate
XIAP	X-linked inhibitor of apoptosis protein

lactate during early-exponential phase and to be capable of faster lactate consumption during late-exponential and stationary phases (Dorai et al., 2009). This is a highly desirable trait for industrial bioprocesses, as a shift to lactate consumption during production phase was found to be a prominent feature of high-titer runs identified through data-mining of 243 production trains at Genentech's Vacaville manufacturing facility (Le et al., 2012). Although it is known that proteins involved in apoptosis regulation may impinge on processes that control mitochondrial energy metabolism (Majors et al., 2007), the effects of these proteins on intracellular metabolic pathways have not been directly studied.

Several alternative approaches have been applied to directly engineer pathways involved in lactate production and energy metabolism, which have been summarized in a recent review (Young, 2013). These studies rely on quantitative analysis of cellular metabolic phenotypes to determine the impact of these genetic manipulations on carbon fluxes. For example, stoichiometric analysis involves the application of mass balances to determine the specific rates and relative ratios of extracellular metabolite transport (Xie and Wang, 1996). This can be useful for assessing nutrient uptake and product excretion by cell cultures. ^{13}C metabolic flux analysis (MFA), on the other hand, leverages this stoichiometric information and combines it with ^{13}C labeling measurements to calculate intracellular metabolic fluxes. ^{13}C MFA has been previously used to map fluxes in both exponential (Ahn and Antoniewicz, 2013; Templeton et al., 2013) and stationary phase (Ahn and Antoniewicz, 2013; Templeton et al., 2013; Sengupta et al., 2011) CHO cultures. However, its application to quantify metabolic alterations in apoptosis-resistant cell lines has not been explored.

In this study, we performed ^{13}C labeling experiments and MFA on a commercially available CHO-S cell line and two apoptosis-resistant clones that were obtained by transfecting the parent CHO-S line with the engineered anti-apoptotic protein Bcl-2Δ. The two clones significantly differed in their level of Bcl-2Δ expression and caspase 3/7 activation. We observed significant rewiring of pyruvate metabolism in both Bcl-2Δ clones, with more pyruvate carbon directed toward mitochondrial oxidation rather than lactate production during the initial phase of growth. This shift in pyruvate metabolism correlated directly with the level of Bcl-2Δ expression observed in each clone. It was also associated with an increase in carbon allocation to biomass relative to lactate in the Bcl-2Δ clones. Eventually, all three cultures shifted from lactate production to consumption, but the apoptosis-resistant clone with the highest Bcl-2Δ expression consumed lactate at an elevated rate compared to the untransfected control. Both Bcl-2Δ clones also exhibited increased activity of mitochondrial enzymes involved in the TCA cycle and oxidative phosphorylation, which may be partially responsible for the observed changes in flux. To the best of our knowledge, this is the first ^{13}C MFA study to quantify the metabolic impacts of anti-apoptosis engineering, enabling a closer examination of the regulatory connections between metabolic and apoptotic pathways.

2. Materials and methods

2.1. Clone generation

A parent CHO-S cell line (Life Technologies, Carlsbad, CA) was transfected with plasmid DNA containing a G418 antibiotic resistance marker to constitutively express Bcl-2Δ. A human CMV promoter was used to achieve high expression of Bcl-2Δ. Plasmid construction was previously described (Dorai et al., 2010). Following G418 selection, approximately 200 clonal populations were generated, and two clones were chosen for further study based upon caspase-3/7 activity. The highest Bcl-2Δ expressing clone (with the lowest caspase-3/7 activity) was designated as the "High-Expressing" (HE) clone, while another clone with moderate caspase activity and less Bcl-2Δ expression was designated as the "Low-Expressing" (LE) clone. The untransfected CHO-S parent was designated as the "Control" line.

2.2. Cell culture

Batch cultures were grown in 125 mL shake flasks at a working volume of 50 mL, using an orbital shaker (145 RPM, 0.45 RCF) inside a humidified incubator maintained at 37 °C and 10% CO_2. Cultures were inoculated at 3×10^5 cells/mL and supplied glucose-free CD-CHO media (Life Technologies, Carlsbad, CA) supplemented with 50 mM glucose and 4 mM glutamine. All growth experiments were carried out for 10 days following inoculation with five separate replicates ($N=5$).

2.3. Caspase-3/7 activity assay

The Apo-ONE homogeneous caspase-3/7 assay (Promega, Madison, WI) was used to assess caspase-3/7 activity. Caspase activity was measured at days 5 and 8 of culture. Cell samples were exposed to rhodamine and lysis buffer for 2 h inside a 37 °C humidified incubator, shaken at 0.08 RCF (155 RPM) on a microplate orbital shaker. Measurements were promptly recorded using a fluorescence plate reader.

2.4. Determination of extracellular exchange rates

Culture samples were collected 2–3 times daily for measurement of specific growth rate and extracellular exchange rates. Viable cell density (VCD) was immediately determined using a trypan blue exclusion method with a Cedex XS automated counter (Roche, Basel, Switzerland). The remainder of the sample was promptly frozen. Glucose and lactate concentrations were determined in culture supernatants using a YSI 2300 biochemical analyzer (YSI, Yellow Springs, OH). Amino acid concentrations were determined using an Agilent 1200 series high performance liquid chromatograph (HPLC). To accurately quantify amino acid concentrations using ultraviolet (UV) absorbance detection, pre-injection derivatization with orthophthaldildehyde (OPA) was used, as described previously (Greene et al., 2009).

The net specific growth rate (μ_{net}), specific death rate (k_d), and gross growth rate (μ_g) were determined by regressing the viable cell density (X) and dead cell density (X_d) measurements using the following equations:

$$\frac{dX}{dt} = \mu_{net} X$$

$$\frac{dX_d}{dt} = k_d X$$

$$\mu_{net} = \mu_g - k_d$$

The specific production rate of extracellular metabolites was determined by regressing the concentration measurements using the following equation:

$$\frac{dC_i}{dt} = q_i X - k_i C_i$$

Here, C_i represents the concentration of the ith measured metabolite, q_i represents its specific production rate (negative if consumed), and k_i is its first-order degradation constant. The only component with a non-negligible chemical degradation rate was glutamine, and its half-life was found to be ~8 days. Regression analysis was performed using the ETA software package (Murphy and Young, 2013).

2.5. Determination of integrated viable cell density (IVCD)

IVCD was determined by trapezoidal integration of the entire measured growth curve, using the following formula:

$$IVCD = \sum_{i=0}^{n} \left[(t_{i+1} - t_i) \left(\frac{X_{i+1} + X_i}{2} \right) \right]$$

where X is viable cell density, t is time, and n is the total number of VCD measurements.

2.6. Isotope labeling experiments

To initiate isotope labeling experiments, cells were centrifuged, washed, and resuspended in CD-CHO media supplemented with a mixture of 50% [1,2-$^{13}C_2$]glucose and 50% [U-$^{13}C_6$] glucose at a total glucose concentration of 50 mM. A minimum of 2.7 days were allowed prior to sampling, as we have previously found that isotopic steady state is achieved in CHO cells after ~2 days of glucose labeling under similar culture conditions (data not shown). Cell culture samples containing approximately 10 million cells were removed and rapidly cold-quenched using a solution of 60% methanol and 40% aqueous ammonium bicarbonate (AMBIC, 0.85% w/v) pre-cooled to −40 °C (Sellick et al., 2009). Cell pellets were extracted using a biphasic chloroform:methanol:water (8:4:3) solution immediately following removal of the quenching solution (Folch et al., 1957). Polar metabolites were recovered in the methanol/water phase.

2.7. Gas chromatography mass spectrometry (GCMS) analysis

Evaporated polar samples were derivatized as described previously (Templeton et al., 2013) and injected into an Agilent 7890 gas chromatograph equipped with a HP5-MS column (30 m × 0.25 mm i.d. × 0.25 μm; Agilent J&W Scientific). Injection volume was varied between 0.2–2 μL, and purge times between 30 and 60 s were used to obtain acceptable signal-to-noise ratios for each fragment ion. The GC outlet was fixed at 270 °C, and helium flow rate was 1 mL/min. The GC oven was initially set at 80 °C and held for 5 min, ramped at 20 °C/min to 140 °C, ramped at 4 °C/min to 280 °C, and held for 5 min. Scan mode allowed all mass spectra between 100–500m/z to be recorded, and raw ion chromatograms were integrated using a custom MATLAB program which applied consistent integration bounds and baseline corrections to each fragment ion (Antoniewicz et al., 2007).

2.8. Reaction network

A reaction network was generated that included all major pathways of central carbon metabolism: glycolysis, pentose phosphate pathway (PPP), TCA cycle, anaplerotic/cataplerotic reactions, amino acid catabolic/anabolic reactions, and a lumped growth reaction. We used the cell composition values from Sheikh et al.

(2005) and determined cell dry weight to be 398, 361, and 343 pg/cell for the control, LE, and HE clone, respectively. This allowed the metabolite yield coefficients included in the lumped growth reaction to be identified (Templeton et al., 2013). Carbon atom transitions and subcellular compartmentation were specified for all reactions. ATP and NAD(P)H balances were not included in the reaction network (Bonarius et al., 1997). In total, there were 116 reactions (including reversible reactions) in the network, 21 extracellular metabolites, and one macromolecular product (biomass). Refer to the Supplementary material for a detailed description of the reaction network and modeling assumptions.

2.9. ^{13}C metabolic flux analysis (MFA)

The INCA analysis platform was used to generate mass balances and isotopomer balances required to simulate ^{13}C labeling within CHO central carbon metabolism (Young, 2014) (accessible at http://mfa.vueinnovations.com/mfa). INCA applies an elementary metabolite unit (EMU) decomposition of the reaction network to efficiently simulate the effects of varying fluxes on the labeling of measurable metabolites (Antoniewicz et al., 2007; Young et al., 2008). We assumed that both metabolic and isotopic quasi-steady-state was obtained during the isotope labeling experiments. Metabolic fluxes were estimated by regression of experimentally determined mass isotopomer distributions (MIDs) and extracellular exchange rates using a Levenberg–Marquardt optimization algorithm. Flux estimation was repeated a minimum of 100 times from random initial values to ensure a global minimum was obtained. All results were subjected to a chi-square statistical test to assess goodness-of-fit, and accurate 95% confidence intervals were computed for all flux parameters by evaluating the sensitivity of the sum-of-squared residuals to parameter variations (Antoniewicz et al., 2006). To effectively visualize the reaction network, flux maps were generated using Cytoscape (Smoot et al., 2011) (accessible at http://www.cytoscape.org).

2.10. Enzyme activity assays

An isocitrate dehydrogenase (IDH) assay kit (Abcam, Cambridge, MA) was used to measure NAD^+ dependent IDH activity of whole CHO cells according to the manufacturer's instructions. Standards and samples were colorimetrically assayed on clear 96-well plates using a Genios plate reader (TECAN, Durham, NC) at 450 nm. A chemiluminescence assay was used to measure Complex I (NADH oxidase) activity in whole CHO cells harvested in PBS. Suspended cells ($5–6 \times 10^5$ cells per well) were placed on white 96-well plates in a solution containing PBS and 20 μM lucigenin. Luminescence was monitored for 5 min using a VICTOR3 plate reader (Perkin–Elmer, Waltham, MA) to establish a baseline reading. Following stimulation with 45 μM NADH, luminescence was monitored for an additional 60 min.

2.11. Western blot

Whole cell protein lysates were collected in RIPA buffer. Following quantification of total protein concentration, 26 μg of total protein was loaded into a 4–20% Tris–HCl gel (Bio-Rad, Hercules, CA). Following electrophoresis and transfer, the membrane was blocked for 100 min with 5% non-fat milk. Next, the membrane was incubated with a Bcl-2 primary antibody that bound to both endogenous Bcl-2 and Bcl-2Δ (Santa Cruz Biotechnology, Santa Cruz, CA). Tubulin was used as a loading control. Incubation with primary antibody was performed at 1:900 (rabbit Bcl-2) and 1:6000 (mouse Tubulin) concentration in 5% non-fat milk for 60 min at room temperature. Incubation with a HRP-labeled secondary antibody (Perkin-Elmer, Waltham, MA) followed, and was performed at 1:1800 (anti-rabbit) and 1:3000 (anti-mouse) concentration in 5% non-fat milk for 60 min at room temperature. To visualize the bands through chemiluminescence, Western Lightning Plus ECL (Perkin-Elmer, Waltham, MA) was used. Image quantification of the blots was performed using ImageJ (Schneider et al., 2012).

2.12. Subcellular localization of Bcl-2 and Bcl-2Δ

Mitochondria-associated endoplasmic reticulum membrane (MAM) samples were prepared as described previously (Vance, 1990). Following homogenization of the cultures grown on 15-cm dishes, the nuclear/whole cell (P1), crude mitochondrial, and microsomal fractions (P3) were prepared by differential centrifugation. Supernatants were collected as the cytosolic fraction. The crude mitochondrial fraction in isolation buffer (250 mM mannitol, 5 mM HEPES, 0.5 mM EGTA, pH 7.4) was subjected to Percoll gradient centrifugation for separation of the MAM from mitochondria. Once all fractions were collected, samples were boiled in 2X sample buffer and analyzed by SDS-PAGE and western blotting.

2.13. Statistical analysis

One-way ANOVA was used to compare the Control, LE, and HE cell lines. If significance was found ($\alpha=0.05$), we applied a Tukey–Kramer test to identify significant differences in mean values. If significance was not found at $\alpha=0.05$, we proceeded to test at $\alpha=0.1$, as noted in the figures.

3. Results

3.1. Clone selection

Two Bcl-2Δ expressing clones were selected that exhibited varying levels of apoptotic resistance based on a screen for caspase-3/7 activity (Fig. 1A). Both clones exhibited significantly reduced caspase-3/7 activity compared to the untransfected control line at day 5 of culture. Western blot analysis revealed that Bcl-2Δ expression was significantly increased in the high-expressing (HE) clone, roughly double that of the low-expressing (LE) clone (Fig. 1B). This result corroborated the result of Fig. 1A, as the HE clone had roughly half the caspase-3/7 activity of the LE clone at the same time point. Increased expression of the endogenous Bcl-2 protein was observed in the LE clone, but the expression level was substantially less than that of Bcl-2Δ (Supplementary Fig. S1). The localization of Bcl-2 was consistent with previously published data (Meunier and Hayashi, 2010), and no differences in the subcellular distribution of Bcl-2 and Bcl-2Δ were observed (Supplementary Fig. S2). To ensure that the relative caspase activity of the clones did not change in a time-dependent manner, we repeated the measurement after approximately 8 days of culture. At this time, we found even more substantially reduced caspase-3/7 activity in both Bcl-2Δ expressing clones in comparison to the control (Supplementary Fig. S3).

3.2. Stoichiometric analysis

To investigate the metabolic consequences of Bcl-2Δ expression, we assessed cell growth rate (Supplementary Fig. S4) and extracellular exchange rates during two separate culture phases by expressing all rates on a C-mol basis (Fig. 2). Due to the fact that lactate flux switched from production to consumption during the course of the culture, an effect often observed in industrial CHO cell cultures (Zagari et al., 2013b), we examined the lactate-producing and lactate-consuming phases separately. These

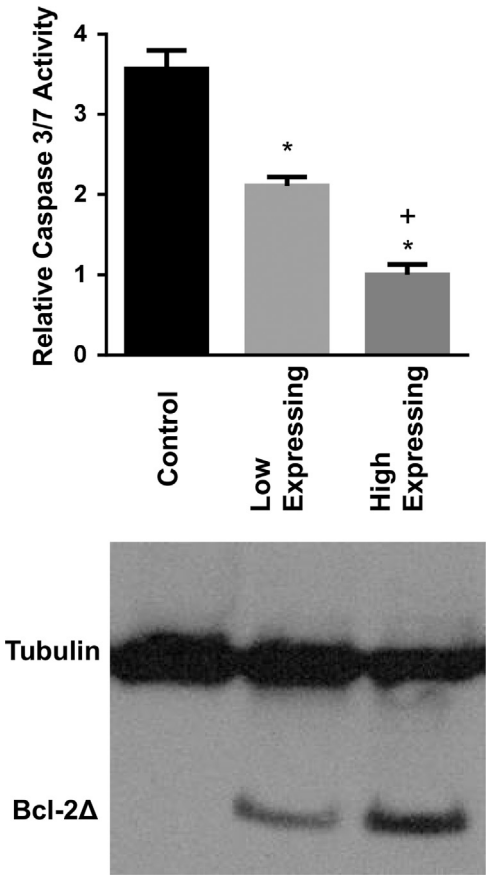

Fig. 1. A. Caspase activity at day 5 of culture. Standard deviation is reported. * Indicates statistically significant difference compared to the control ($p=0.05$). + Indicates statistically significant difference between Low Expressing and High Expressing clones ($p=0.05$). B. Western blot for Bcl-2Δ at day 5 of culture. The primary antibody bound to both endogenous Bcl-2 and engineered Bcl-2Δ. Bcl-2Δ expression was substantially greater than Bcl-2, explaining why only one band was visible. For further confirmation of Bcl-2/Bcl-2Δ expression level, refer to Supplementary Fig. S1.

corresponded roughly with the exponential and stationary phases, as previously reported in literature (Ahn and Antoniewicz, 2011).

3.2.1. Lactate-producing phase

In the lactate-producing phase (Fig. 2A), the HE clone produced lactate at a rate that was approximately half that of the control. Alanine production also fell significantly in both the HE and LE clones. Biomass production was the only other substantial carbon output during this phase, with a magnitude comparable to lactate on a C-mol basis. However, while the control clone produced only 0.92 ± 0.11 C-mol of biomass for every 1 C-mol of lactate, the HE clone was 27% more efficient in its carbon utilization, producing 1.17 ± 0.15 C-mol of biomass for every 1 C-mol of lactate (Fig. 2B). In terms of carbon inputs, the HE clone consumed glucose at a significantly lower rate than the LE clone and nearly a third less compared to the control. Glutamine consumption was significantly reduced in both Bcl-2Δ expressing clones. In general, amino acid consumption was reduced in both Bcl-2Δ expressing clones, but with the exception of glutamine, none of the other amino acid fluxes contributed substantially to the overall carbon balance.

Examination of the culture growth rates reveals further insight into the metabolic impact of Bcl-2Δ expression. The HE clone had a growth rate that was significantly reduced by 16% compared to the control (Supplementary Fig. S4). Previous work has found Bcl-2 overexpression to have a similar negative impact on growth (Simpson et al., 1999). However, the LE clone did not differ significantly from the control in growth rate despite diminished lactate production and reduced glucose consumption (Fig. 2A). This indicates that the reduction in nutrient uptake and lactate production in the LE clone reflects a direct effect of Bcl-2Δ expression on metabolic pathways rather than a growth-rate-dependent effect. Furthermore, the total incoming carbon flux was reduced by approximately 10% in the LE clone and by 30% in the HE clone during the lactate-producing phase (Fig. 3).

3.2.2. Lactate-consuming phase

The lactate-consuming phase was notably different from the lactate-producing phase. The sum of the specific lactate and glucose consumption rates accounted for 79–89% of the total carbon consumed in the three clones. Outgoing carbon flux to biomass was limited during this phase, but was not negligible. Nearly all of the extracellular carbon substrates were consumed during this phase, including several metabolites previously excreted during the lactate-producing phase. Incoming lactate flux was significantly higher in the HE line, while the LE clone consumed lactate at nearly the same rate as the control (Fig. 2C). However, the glucose uptake rate was significantly reduced in both Bcl-2Δ expressing clones. The lactate-to-glucose ratio was 54% greater in the HE clone when compared to the control (Supplementary Fig. S5). Thus incoming lactate flux made up a significantly greater fraction of the total incoming carbon flux in the HE clone, a 44% increase compared to the control (Fig. 2D). As expected, the culture was considerably less metabolically active relative to the lactate-producing phase, as indicated by drastic reductions in total carbon consumption (Fig. 3).

3.3. ^{13}C metabolic flux analysis (^{13}C MFA)

With significant rerouting of extracellular fluxes observed during both the lactate-producing and lactate-consuming phases, we sought to identify the fate of the incoming glucose carbon and to quantify the intracellular flux distributions of all three clones. We performed a ^{13}C labeling study followed by metabolic flux analysis (MFA) to calculate intracellular metabolic fluxes in both the lactate-producing and lactate-consuming phases.

3.3.1. Lactate-producing phase

The flux maps obtained by ^{13}C MFA during the lactate-producing phase are shown in Fig. 4. A few notable features are shared by all three clones. Minimal oxidative pentose phosphate pathway (oxPPP) activity was observed, and nearly all of the glucose consumed was directed through glycolysis to pyruvate. This result has been observed in previous ^{13}C MFA studies of exponential-phase CHO cultures (Ahn and Antoniewicz, 2013). Flux through malic enzyme (ME) was the most substantial cataplerotic flux leaving the TCA cycle during this phase. Still, nearly all of the pyruvate generated was attributable to the pyruvate kinase (PK) flux. A substantial portion of the pyruvate generated was converted into lactate; however, the HE clone diverted less pyruvate toward lactate production than the other cell lines.

Despite decreased total carbon consumption by both Bcl-2Δ expressing clones (Fig. 3), TCA cycle fluxes were not significantly different among the three cell lines. Therefore, we examined how the incoming carbon was partitioned at the pyruvate node to maintain consistent TCA cycle activity, since pyruvate is a central metabolic hub where fermentative and oxidative pathways bifurcate. To this end, we compared all incoming and outgoing pyruvate fluxes at the pyruvate node (Fig. 5). In the control line, $33 \pm 7\%$ of

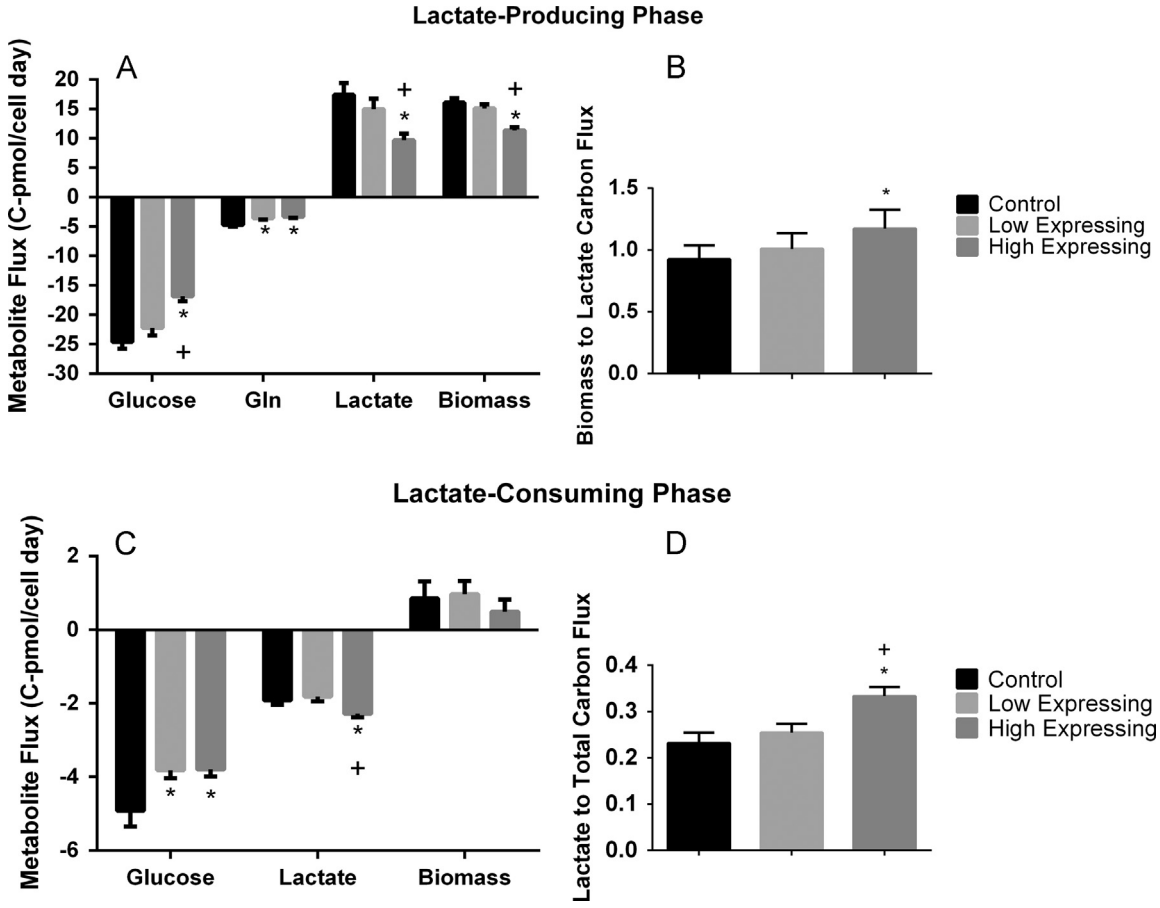

Fig. 2. Major extracellular carbon fluxes. Carbon flux is determined by multiplying the flux (specific uptake rate, production rate) by the number of carbons in the molecule. Standard deviation is reported. * Indicates statistically significant difference compared to the control ($p=0.05$).+Indicates statistically significant difference between Low Expressing and High Expressing clones ($p=0.05$). A. Fluxes during the lactate-producing phase. The biomass carbon output corresponded with the following gross growth rates: Control 1.00 ± 0.04 day^{-1}, Low Expressing 0.99 ± 0.04 day^{-1}, and High Expressing 0.84 ± 0.03 day^{-1}. B. Ratio of biomass to lactate carbon fluxes during the lactate-producing phase. C. Fluxes during the lactate-consuming phase. The biomass carbon output corresponded with the following gross growth rates: Control 0.05 ± 0.02 day^{-1}, Low Expressing 0.06 ± 0.01 day^{-1}, and High Expressing 0.03 ± 0.01 day^{-1}. D. Ratio of incoming lactate carbon flux to total incoming carbon flux during the lactate-consuming phase.

carbon leaving the pyruvate node was transferred to the mitochondria through pyruvate carboxylase (PC) and pyruvate dehydrogenase (PDH). However, as Bcl-2Δ expression level increased, a greater fraction of the incoming pyruvate was directed to the mitochondria, reaching as high as $44 \pm 7\%$ in the HE clone.

With a higher fraction of pyruvate oxidized in mitochondria, we hypothesized that more mitochondrial NADH would be generated per glucose consumed and more oxidative metabolism would be detected in the Bcl-2Δ expressing clones. To test this hypothesis, and to identify a potential mechanism by which the Bcl-2Δ cells increased their mitochondrial activity, we measured the enzymatic activities of the mitochondrial enzymes isocitrate dehydrogenase (IDH) and NADH-coenzyme Q oxidoreductase (Complex I). IDH is a rate-controlling step in the TCA cycle that catalyzes the oxidative conversion of citrate to alpha-ketoglutarate, with concomitant evolution of CO_2 and generation of NADH. As indicated in Fig. 6A, the IDH activity was at least 60% higher in both engineered cell lines relative to the control, which indicates a shift toward increased oxidative capacity in response to Bcl-2Δ expression. Similarly, both Bcl-2Δ expressing clones were determined to have significantly increased Complex I activity (Fig. 6B). This enzyme functions to oxidize NADH produced in the TCA cycle and is a vital component of the mitochondrial electron transport chain.

3.3.2. *Lactate-consuming phase*

During the lactate-consuming phase, growth slowed dramatically and the total incoming carbon flux decreased by nearly an order of magnitude. This was due largely to decreased glucose consumption rates as all 3 clones transitioned into stationary phase (Fig. 2C). Past work has found similar reductions in glucose flux following a switch to lactate consumption (Li et al., 2012). The majority of incoming glucose was diverting to the oxPPP, with fluxes ranging from 76% of total carbon uptake in the control line to 61% in the HE clone (Fig. 7). Even so, the TCA cycle was the main focal point of central metabolism during the lactate-consuming phase, with the majority of incoming carbon ultimately directed there for oxidation to CO_2.

Fig. 8 shows the distribution of carbon fluxes entering the pyruvate node during this phase. Most of the incoming pyruvate carbon can be broken down into two components: the contribution from lactate and the contribution from glycolysis. Lactate accounted for $39 \pm 1\%$ of the input carbon in the HE clone compared to only $29 \pm 4\%$ in the control line. The LE clone fell in the middle at $35 \pm 5\%$. Whether viewed on an absolute (Fig. 2C) or relative basis (Fig. 8), the utilization of lactate by the HE clone is significantly greater than the control. Since all of the outgoing flux from pyruvate was directed to the mitochondria during this phase, we again became interested in whether changes in carbon

partitioning at the pyruvate node were associated with changes in mitochondrial oxidative capacity. Therefore, we measured IDH activity (Fig. 6A) and Complex I activity (Fig. 6B) in cells harvested during the lactate-consuming phase. As in the lactate-producing phase, the activities of both mitochondrial enzymes were significantly higher in the Bcl-2Δ expressing clones as compared to the control.

4. Discussion

Bcl-2 was originally known for its role as an oncogene, having been frequently found overexpressed in several different cancer cell types (Placzek et al., 2010)—most notably B-cell lymphoma for which it is named. More recently, the biotechnology industry became interested in Bcl-2 and other anti-apoptotic genes due to their ability to increase survival of industrial cell lines with a potential impact on enhancing product yields (Chiang and Sisk, 2005; Figueroa et al., 2001; Meents et al., 2002). In 2000, multiple laboratories including our group (Mastrangelo et al., 2000; Tey et al., 2000) found that Bcl-2 expression indeed retards apoptotic progression in CHO cells, including those producing recombinant proteins. Dorai et al. (2009) later observed that antibody-producing CHO cells engineered to overexpress a variety of different anti-apoptotic genes exhibited less lactate accumulation during early exponential phase and more rapid lactate consumption during late exponential and stationary phases.

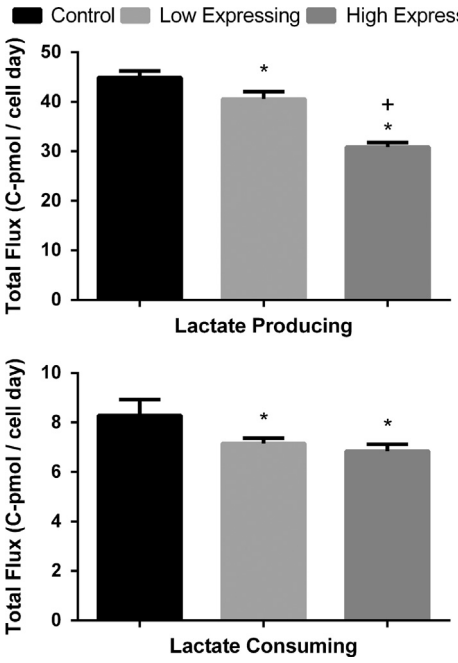

Fig. 3. Total incoming carbon flux during each phase. Standard deviation is reported. * Indicates statistically significant differences compared to the control ($p=0.05$).+Indicates statistically significant differences between the Low Expressing and High Expressing clones ($p=0.05$).

The current study builds upon this previous work to examine the metabolic response of CHO cells to recombinant expression of Bcl-2Δ, an engineered variant of Bcl-2 where both the BH2 and BH3 motifs have been removed. This serves to enhance protein stability, since several ubiquitination sites and regulatory motifs have been removed from the truncated sequence (Figueroa et al., 2001). Expression of Bcl-2Δ in CHO cells has been previously shown to surpass wild-type Bcl-2 in its ability to extend culture survival in response to diverse insults (Figueroa et al., 2001). In this study, the expression of Bcl-2Δ was greatly enhanced in our clones relative to the endogenous Bcl-2 level of control cells (Supplementary Fig. S1), presumably due to both the use of a strong constitutive CMV promoter and the increased stability of Bcl-2Δ. This resulted in rewiring of metabolic fluxes at the pyruvate node, both during the lactate-producing and lactate-consuming phases of culture. We sought to better understand the regulatory connections between these metabolic alterations and the known anti-apoptotic properties of Bcl-2.

Bcl-2 is known to regulate cell death by modulating mitochondrial membrane permeability (Tait and Green, 2010) and is believed to function by preventing the release of cytochrome c from the intramembrane space, which is a committed step in several different apoptotic mechanisms (Wei et al., 2008). There are multiple hypotheses surrounding how mitochondrial permeability is regulated by Bcl-2, as discussed in a recent review (Lewis et al., 2013). Some evidence supports a role for Bcl-2 in blocking permeability transition pore (PTP) activation, thus preventing

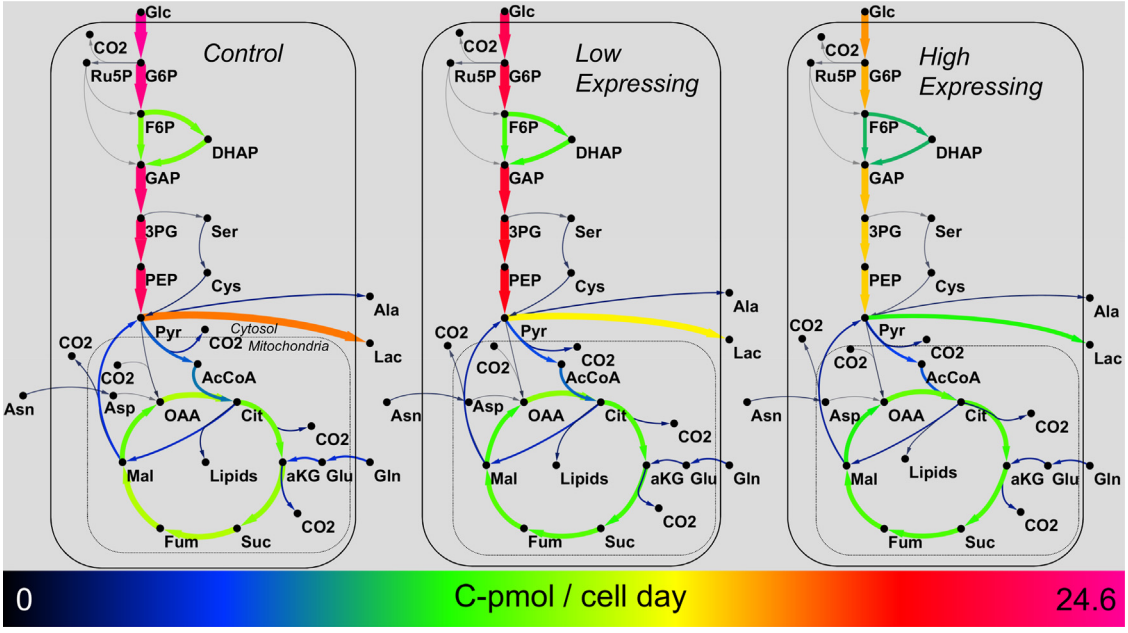

Fig. 4. Metabolic flux maps during the lactate-producing phase. The magnitude of each net carbon flux corresponds with the color and width of the reaction arrow.

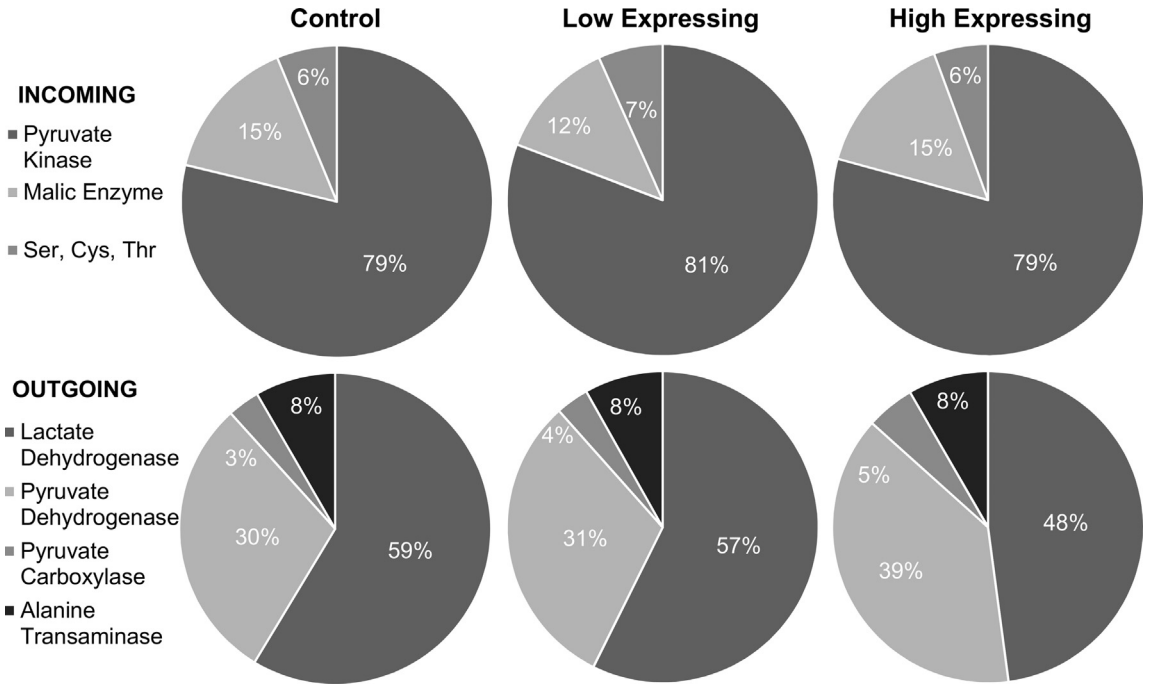

Fig. 5. Distribution of flux at the pyruvate node during the lactate-producing phase. Cys, Ser, Thr represents the summed contributions of these three amino acids to pyruvate production.

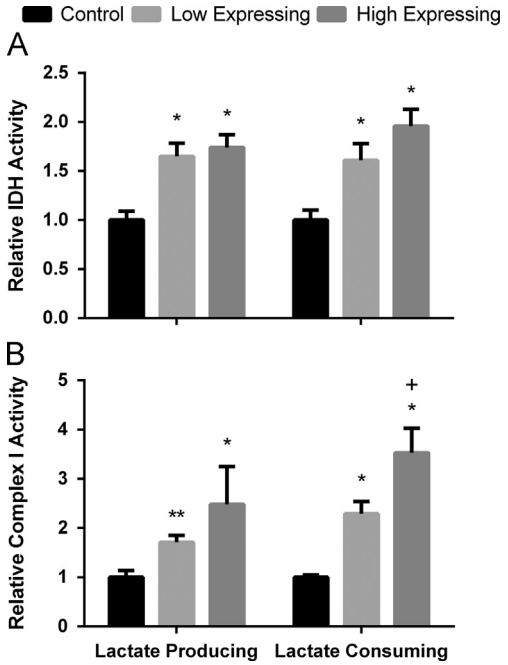

Fig. 6. Enzyme activity assays. A. Relative enzymatic activity of isocitrate dehydrogenase (IDH). B. Relative enzymatic activity of Complex I (NADH oxidase). Standard deviation is reported. * Indicates statistically significant difference compared to the control ($p=0.05$).+Indicates statistically significant difference between the Low Expressing and High Expressing clones ($p=0.05$). Comparisons of both assays are relative to the control enzymatic activity, and are only appropriate when compared within a specific phase (i.e., within the lactate-producing phase or lactate-consuming phase). ** Indicates statistically significant difference compared to the control ($p=0.1$).

dissipation of inner mitochondrial transmembrane potential ($\Delta\psi_m$) (Murphy et al., 2001; Gupta et al., 2010). Bcl-2 has also been found to limit activity of the voltage-dependent anion channel (VDAC), a protein essential to the regulation of mitochondrial Ca^{2+} uptake (Orrenius et al., 2003). These effects would be expected to simultaneously modulate metabolic pathway activities, since several mitochondrial enzymes are regulated by changes in Ca^{2+} and $\Delta\psi_m$ (Majors et al., 2007). These include IDH and Complex I enzymes that catalyze important redox reactions in the TCA cycle and oxidative phosphorylation (OXPHOS), respectively. Furthermore, the effect of Bcl-2 to prevent loss of cytochrome c from the intramembrane space may also function to regulate OXPHOS, as cytochrome c is a required part of the mitochondrial electron transport chain.

Our measurements indicate that Bcl-2Δ expression increased enzymatic activities of both IDH and Complex I (Fig. 6), potentially enhancing mitochondrial oxidative capacity. The effect was accompanied by a greater fraction of pyruvate produced during the lactate-producing phase being directed to the mitochondria for oxidation (Fig. 5). In addition, there was a significant increase in the lactate consumption rate (Fig. 2C) and a significant increase in the fraction of pyruvate carbon derived from lactate (Fig. 8) during the lactate-consuming phase. We hypothesize that these systems-level metabolic alterations stem, at least in part, from the changes in mitochondrial enzymatic activities we observed.

Bcl-2 has also been shown to enhance the activity of several Ca^{2+}-dependent mitochondrial transporters, including adenine nucleotide translocator (ANT) (Belzacq et al., 2003). ANT exists in the inner mitochondrial membrane and enables exchange of ADP/ATP with the cytosol. Lack of mitochondrial ADP availability could lead to a potential bottleneck within the OXPHOS pathway of control cells. Removal of this bottleneck could be another potential explanation for the increased pyruvate shuttled to the mitochondria and enhanced Complex I activity observed in the HE clone. Others have found that there is a limitation in the Ca^{2+}-dependent Asp/Glu transporter of CHO cells, which is responsible for transport of NAD^+ equivalents into the cytosol as part of the malate-aspartate shuttle (Zagari et al., 2013a; Lasorsa et al., 2003). This could explain the reduced lactate production observed in the Bcl-2Δ clones, since the conversion of pyruvate to lactate by lactate dehydrogenase (LDH) provides an alternative pathway to oxidize NADH that is expected to become less important as mitochondrial OXPHOS and malate-aspartate shuttle capacities increase. Based

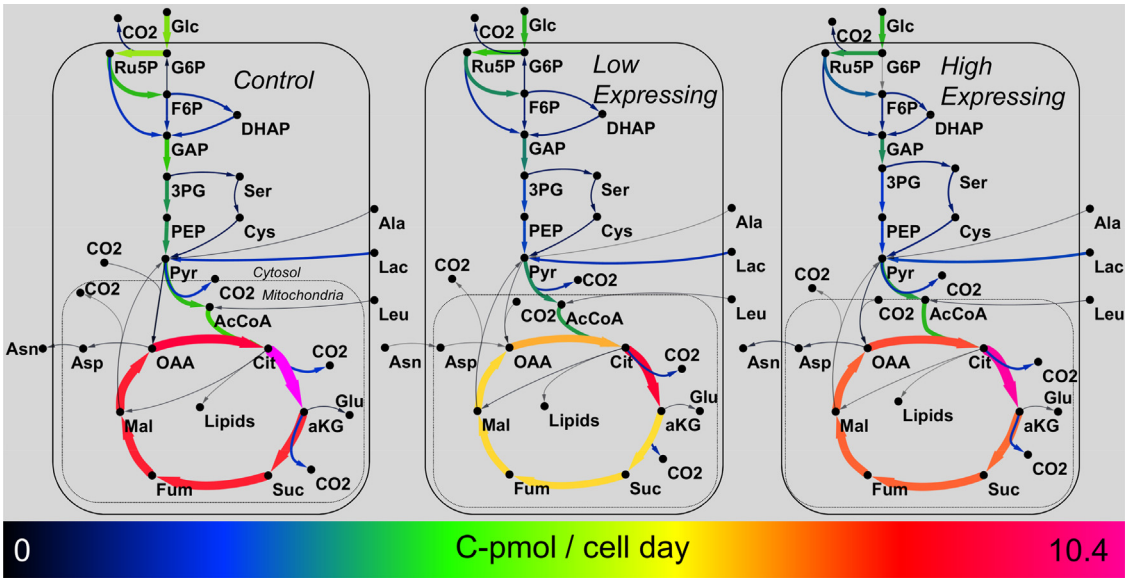

Fig. 7. Metabolic flux map of lactate-consuming phase. The magnitude of each net carbon flux corresponds with the color and width of each reaction arrow.

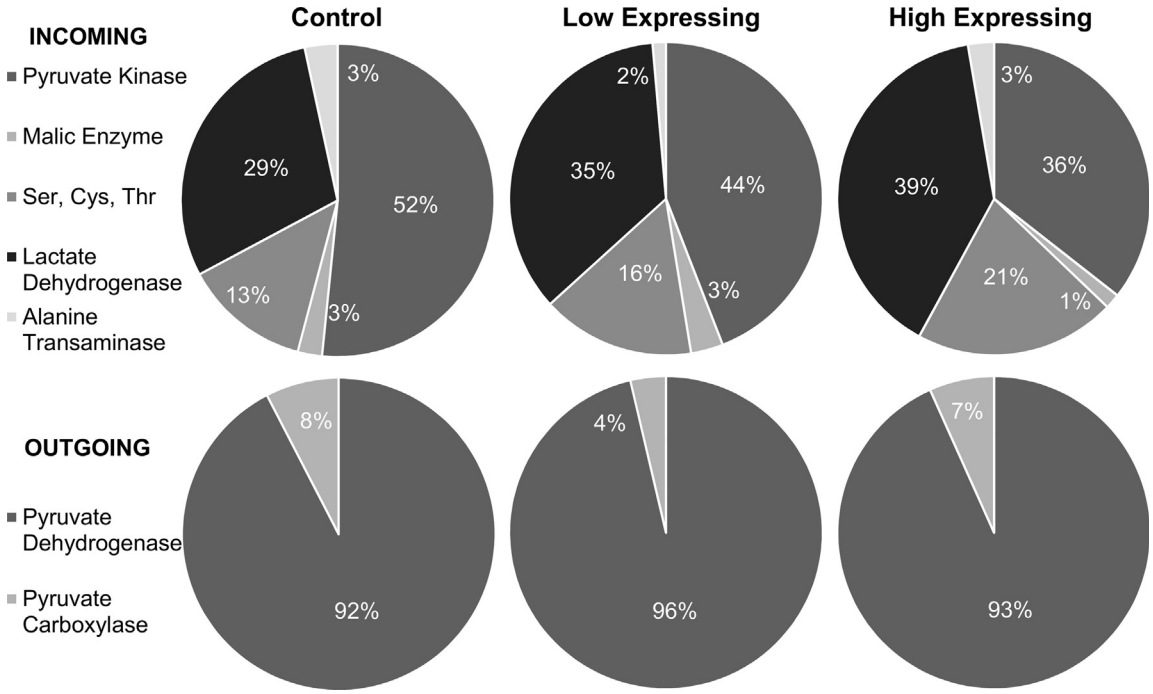

Fig. 8. Distribution of carbon flux at the pyruvate node during the lactate-consuming phase.

upon the lactate/glucose ratio, both Bcl-2Δ expressing clones exhibited reduced reliance on lactate production for maintaining cytosolic redox during the lactate-producing phase (Supplementary Fig. S5). Likewise, the enhanced lactate consumption exhibited by the HE clone after the lactate shift may be partially explained by increased mitochondrial transport and disposal of NADH equivalents generated by LDH acting in the reverse direction. Taken together, the known role of anti-apoptotic proteins such as Bcl-2 to alter mitochondrial Ca^{2+} flux and $\Delta\psi_m$ are important for regulating several aspects of mitochondrial metabolism that could explain our observations.

Even though recombinant expression of Bcl-2Δ did not positively impact the growth rate, it did clearly hinder the progression of cell death. Bcl-2Δ expression led to increases in IVCD of 40% in the HE culture and 20% in the LE culture (Fig. 9). This is in agreement with prior studies where Bcl-2 was found to inhibit cell death without increasing cell proliferation (Vaux et al., 1988; Youle and Strasser, 2008). Peak VCD was also increased by nearly 50% in the HE clone and nearly 40% in the LE clone (Supplementary Fig. S6). This reflects an increase in biomass yield, as the Bcl-2Δ expressing cells directed more carbon flux to biomass production rather than lactate (Fig. 2B). Additionally, glutamine consumption decreased significantly in the Bcl-2Δ clones, perhaps attributable to the redistribution of pyruvate carbon to the TCA cycle. This increased carbon efficiency is likely a result of enhanced TCA cycle activity relative to glycolysis, since OXPHOS provides more ATP per glucose consumed than lactate production. Further evidence for this increased carbon efficiency is reflected in the fact that the reductions in growth rate observed in both Bcl-2Δ clones (HE down 16%; LE unaffected) was substantially less than the

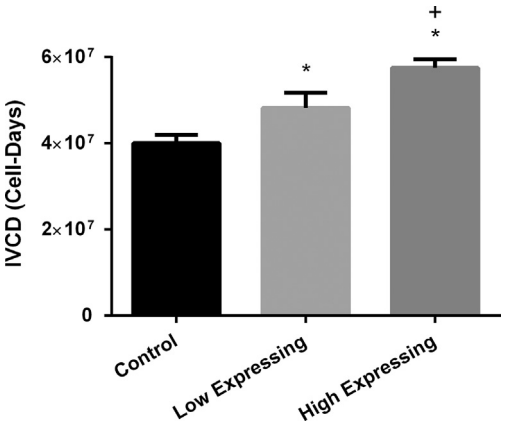

Fig. 9. Integrated viable cell density (IVCD) over the culture life. Standard deviation is reported. * Indicates statistically significant difference compared to the control ($p=0.05$).+Indicates statistically significant difference between the Low Expressing and High Expressing clones ($p=0.05$).

reductions in their total carbon consumption rate (HE down 30%; LE down 10%).

In addition to the enhancements in biomass yield, the accompanying reduction in lactate production would be expected to have further benefits in an industrial bioprocess, since elevated lactate concentrations have been found to hamper both growth and antibody production of CHO cell cultures (Lao and Toth, 1997). The HE line allowed lactate to accumulate to marginally less ($<10\%$) concentrations than the control, despite achieving $\sim$50% higher peak VCD (Supplementary Figs. S6 and S7). Furthermore, a culture capable of consuming the lactate that it previously produced is at an obvious advantage in a controlled bioreactor. A lactate-consuming culture requires less base addition to maintain pH and results in less rise in osmolarity (Chen et al., 2001), which has also been found to negatively affect growth. All cell lines examined in this study consumed previously produced lactate; however, the HE clone consumed lactate at a specific rate significantly greater than the others, confirming the result that Dorai et al. (2009) obtained in their apoptosis-resistant lines.

Although prior work by Meents et al. (2002) found that Bcl-2 overexpression did not increase specific protein productivity, Bcl-2Δ clones have the potential to outperform Bcl-2 overexpressing clones in terms of protein production (Figueroa et al., 2001; Meents et al., 2002). While the current study did not address the effects of Bcl-2Δ expression on protein production, recent work from our group has found a strong correlation between enhanced TCA cycling and peak antibody production (Templeton et al., 2013). Therefore, we expect that anti-apoptosis engineering may offer a path toward improving specific protein productivity while reducing lactate accumulation and improving biomass yields, in addition to its well-known effects to extend culture longevity.

The ^{13}C flux analysis performed in this study was dependent on assumptions of both isotopic and metabolic steady states. Although we did not obtain biomass samples during the initial two days of growth due to the low cell densities achieved during this period, multiple parallel experiments where tracers were administered to higher density cultures indicate that the ^{13}C enrichment of intracellular metabolites plateaus after $\sim$2 days of labeling. Therefore, all samples used for ^{13}C isotopomer analysis were collected following more than two days of labeling, which we expect to be sufficient to achieve isotopic steady state. It is also possible that the metabolic steady-state assumption was violated due to dynamic changes that occur during the transition from lactate-producing to lactate-consuming phases of culture. While this is indeed a concern, there are currently no established methods for performing fully dynamic ^{13}C MFA under metabolic nonstationary conditions (Ahn and Antoniewicz, 2012; Antoniewicz, 2013). Therefore, in order to address industrially relevant culture conditions where metabolism is changing over time, it is necessary to invoke a quasi-steady-state assumption. This involves the premise that, after the initial tracer equilibration period, further changes in isotope labeling will track closely with changes in metabolism and can be analyzed by steady-state ^{13}C MFA to obtain a series of snapshots that describes the variation in metabolic fluxes over time. This is similar to the approach used by Antoniewicz et al. (2007) to profile dynamic changes in *E. coli* metabolism during a fed-batch culture that exhibited both glycerol-producing and glycerol-consuming phases. Despite these limitations and assumptions, we expect that the ^{13}C MFA results are reliable because (i) the main findings related to pyruvate partitioning are consistent with extracellular flux measurements and with direct measurements of mitochondrial enzyme activities, (ii) the enrichments of pyruvate and lactate were maintained near their maximal levels throughout both phases of culture, (iii) we did not utilize samples collected immediately following the lactate shift, and (iv) the average ^{13}C enrichments of metabolites from the control and HE lines were consistent within each phase, despite being collected at different times due to the delayed onset of lactate consumption in the HE culture (Supplementary Fig. S8).

5. Conclusions

Host cell engineering through recombinant Bcl-2Δ expression has considerable potential for industrial applications. It notably improves the total IVCD by delaying the onset of apoptosis. In addition, this study has shown that Bcl-2Δ expression promotes a shift toward increased mitochondrial oxidation of incoming carbon substrates. Bcl-2Δ's ability to limit lactate production and enhance lactate consumption is an especially attractive property, and will only become more so, as industry continues to push toward higher peak VCDs and longer culture lifespans. To the best of our knowledge, this is the first ^{13}C MFA study to quantify the metabolic impact of Bcl-2Δ expression, enabling a closer examination of the interplay between apoptotic and metabolic regulatory functions of Bcl-2Δ through comprehensive analysis of central carbon metabolism.

Acknowledgments

This work was supported by NSF GOALI award CBET-1067766. The authors would like to acknowledge the contributions from Dawn Ellis in clone generation. The authors would also like to thank Daniel Wolozny for his general assistance in this study.

Appendix A. Supporting information

Supplementary data associated with this article can be found in the online version at http://dx.doi.org/10.1016/j.ymben.2014.06.010.

References

Aggarwal, S.R., 2012. What's fueling the biotech engine-2011 to 2012. Nat. Biotechnol. 30 (12), 1191–1197 (Dec.).
Ahn, W.S., Antoniewicz, M.R., 2011. Metabolic flux analysis of CHO cells at growth and non-growth phases using isotopic tracers and mass spectrometry. Metab. Eng. 13 (5), 598–609 (Sep).
Ahn, W.S., Antoniewicz, M.R., 2012. Towards dynamic metabolic flux analysis in CHO cell cultures.,. Biotechnol. J. 7 (1), 61–74 (Jan.).
Ahn, W.S., Antoniewicz, M.R., 2013. Parallel labeling experiments with [1,2-(13)C] glucose and [U-(13)C]glutamine provide new insights into CHO cell metabolism. Metab. Eng. 15, 34–47 (Jan).

Altamirano, C., Paredes, C., Illanes, a, Cairó, J.J., Gòdia, F., 2004. Strategies for fed-batch cultivation of t-PA producing CHO cells: substitution of glucose and glutamine and rational design of culture medium. J. Biotechnol. 110 (2), 171–179 (May).
Antoniewicz, M.R., 2013. Dynamic metabolic flux analysis – tools for probing transient states of metabolic networks. Curr. Opin. Biotechnol. 24 (6), 973–978 (Dec.).
Antoniewicz, M.R., Kelleher, J.K., Stephanopoulos, G., 2006. Determination of confidence intervals of metabolic fluxes estimated from stable isotope measurements. Metab. Eng. 8 (4), 324–337 (Jul.).
Antoniewicz, M.R., Kelleher, J.K., Stephanopoulos, G., 2007. Elementary metabolite units (EMU): a novel framework for modeling isotopic distributions. Metab. Eng. 9 (1), 68–86 (Jan).
Antoniewicz, M.R., Kraynie, D.F., Laffend, L.a., González-Lergier, J., Kelleher, J.K., Stephanopoulos, G., 2007. Metabolic flux analysis in a nonstationary system: fed-batch fermentation of a high yielding strain of E. coli producing 1,3-propanediol. Metab. Eng. 9 (3), 277–292 (May).
Belzacq, A., Vieira, H.L.A., Verrier, F., Cohen, I., Larquet, E., Pariselli, F., Petit, P.X., Kahn, A., Rizzuto, R., Brenner, C., Kroemer, G., 2003. Bcl-2 and Bax modulate adenine nucleotide translocase activity Bcl-2 and Bax modulate adenine nucleotide translocase activity 1. Cancer Res. 63, 541–546.
Bonarius, H., Schmid, G., Tramper, J., 1997. Flux analysis of underdetermined metabolic networks: the quest for the missing constraints. Trends Biotechnol. 15 (8), 308–314 (Aug.).
Chen, K., Liu, Q., Xie, L., Sharp, P.a., Wang, D.I., 2001. Engineering of a mammalian cell line for reduction of lactate formation and high monoclonal antibody production. Biotechnol. Bioeng. 72 (1), 55–61 (Jan.).
Chiang, G.G., Sisk, W.P., 2005. Bcl-x(L) mediates increased production of humanized monoclonal antibodies in Chinese hamster ovary cells. Biotechnol. Bioeng. 91 (7), 779–792 (Sep.).
Dorai, H., Kyung, Y.S., Ellis, D., Kinney, C., Lin, C., Jan, D., Moore, G., Betenbaugh, M.J., 2009. Expression of anti-apoptosis genes alters lactate metabolism of Chinese hamster ovary cells in culture. Biotechnol. Bioeng. 103 (3), 592–608 (Jun.).
Dorai, H., Ellis, D., Keung, Y.S., Campbell, M., Zhuang, M., Lin, C., Betenbaugh, M.J., 2010. Combining high-throughput screening of caspase activity with anti-apoptosis genes for development of robust CHO production cell lines. Biotechnol. Prog. 26 (5), 1367–1381.
Farid, S.S., 2007. Process economics of industrial monoclonal antibody manufacture. J. Chromatogr. B. Analyt. Technol. Biomed. Life Sci. 848 (1), 8–18 (Mar.).
Figueroa, B., Sauerwald, T.M., Mastrangelo, A.J., Hardwick, J.M., Betenbaugh, M.J., 2001. Comparison of Bcl-2 to a Bcl-2 deletion mutant for mammalian cells exposed to culture insults. Biotechnol. Bioeng. 73 (3), 211–222 (May).
Folch, J., Lees, M., Stanley, G.H.S., 1957. A simple method for the isolation and purification of total lipides from animal tissues. J. Biol. Chem. 226 (1), 497–509 (Aug).
Fussenegger, M., Fassnacht, D., Schwartz, R., Zanghi, J.a., Graf, M., Bailey, J.E., Pörtner, R., 2000. Regulated overexpression of the survival factor bcl-2 in CHO cells increases viable cell density in batch culture and decreases DNA release in extended fixed-bed cultivation.,. Cytotechnology 32 (1), 45–61 (Jan.).
Goswami, J., Sinskey, a.J., Steller, H., Stephanopoulos, G.N., Wang, D.I.C., 1999. Apoptosis in batch cultures of Chinese hamster ovary cells. Biotechnol. Bioeng. 62 (6), 632–640 (Mar.).
Greene, J., Henderson, J.W., Jr. Wikswo, J.P., 2009. Rapid and precise determination of cellular amino acid flux rates using HPLC with automated derivatization with absorbance detection. Application Note 5990-3283EN, Agilent Technologies.
Gupta, S., Cuffe, L., Szegezdi, E., Logue, S.E., Neary, C., Healy, S., Samali, A., 2010. Mechanisms of ER stress-mediated mitochondrial membrane permeabilization. Int. J. Cell Biol. 2010, 170215 (Jan.).
Lao, M.S., Toth, D., 1997. Effects of ammonium and lactate on growth and metabolism of a recombinant Chinese hamster ovary cell culture. Biotechnol. Prog. 13 (5), 688–691.
Lasorsa, F.M., Pinton, P., Palmieri, L., Fiermonte, G., Rizzuto, R., Palmieri, F., 2003. Recombinant expression of the Ca(2+)-sensitive aspartate/glutamate carrier increases mitochondrial ATP production in agonist-stimulated Chinese hamster ovary cells. J. Biol. Chem. 278 (40), 38686–38692 (Oct.).
Le, H., Kabbur, S., Pollastrini, L., Sun, Z., Mills, K., Johnson, K., Karypis, G., Hu, W.-S., 2012. Multivariate analysis of cell culture bioprocess data – lactate consumption as process indicator. J. Biotechnol. 162 (2–3), 210–223 (Dec.).
Lewis, A., Hayashi, T., Su, T., Betenbaugh, M.J., 2013. Bcl-2 family in inter-organelle modulation of calcium signaling; roles in bioenergetics and cell survival. J. Bioenerg. Biomembr. (Sep.).
Li, J., Wong, C.L., Vijayasankaran, N., Hudson, T., Amanullah, A., 2012. Feeding lactate for CHO cell culture processes: impact on culture metabolism and performance. Biotechnol. Bioeng. 109 (5), 1173–1186 (May).
Majors, B.S., Betenbaugh, M.J., Chiang, G.G., 2007. Links between metabolism and apoptosis in mammalian cells: applications for anti-apoptosis engineering. Metab. Eng. 9 (4), 317–326 (Jul.).
Mastrangelo, A.J., Hardwick, J.M., Zou, S., Betenbaugh, M.J., 2000. Part II. Overexpression of bcl-2 family members enhances survival of mammalian cells in response to various culture insults. Biotechnol. Bioeng. 67 (5), 555–564 (Mar).
Mastrangelo, A.J., Zou, S., Hardwick, J.M., Betenbaugh, M.J., 1999. Antiapoptosis chemicals prolong productive lifetimes of mammalian cells upon Sindbis virus vector infection. Biotechnol. Bioeng. 65 (3), 298–305 (Nov).
Meents, H., Enenkel, B., Eppenberger, H.M., Werner, R.G., Fussenegger, M., 2002. Impact of coexpression and coamplification of sICAM and antiapoptosis determinants bcl-2/bcl-x(L) on productivity, cell survival, and mitochondria number in CHO-DG44 grown in suspension and serum-free media. Biotechnol. Bioeng. 80 (6), 706–716 (Dec.).
Meunier, J., Hayashi, T., 2010. Sigma-1 receptors regulate Bcl-2 expression by reactive oxygen species-dependent transcriptional regulation of nuclear factor kappa B. J. Pharmacol. Exp. Ther. 332 (2), 388–397.
Murphy, R.C., Schneider, E., Kinnally, K.W., 2001. Overexpression of Bcl-2 suppresses the calcium activation of a mitochondrial megachannel. FEBS Lett. 497 (2–3), 73–76 (May).
Murphy, T.A., Young, J.D., 2013. ETA: robust software for determination of cell specific rates from extracellular time courses. Biotechnol. Bioeng. 110 (6), 1748–1758 (Jun.).
Orrenius, S., Zhivotovsky, B., Nicotera, P., 2003. Regulation of cell death: the calcium-apoptosis link. Nat. Rev. Mol. Cell Biol. 4 (7), 552–565 (Jul.).
Placzek, W.J., Wei, J., Kitada, S., Zhai, D., Reed, J.C., Pellecchia, M., 2010. A survey of the anti-apoptotic Bcl-2 subfamily expression in cancer types provides a platform to predict the efficacy of Bcl-2 antagonists in cancer therapy. Cell Death Dis. 1 (5), e40 (Jan.).
Schneider, C.A., Rasband, W.S., Eliceiri, K.W., 2012. NIH Image to ImageJ: 25 years of image analysis. Nat. Methods 9 (7), 671–675 (Jun).
Sellick, C.A., Hansen, R., Maqsood, A.R., Dunn, W.B., Stephens, G.M., Goodacre, R., Dickson, A.J., 2009. Effective quenching processes for physiologically valid metabolite profiling of suspension cultured mammalian cells. Anal. Chem. 81 (1), 174–183 (Jan).
Sengupta, N., Rose, S.T., Morgan, J.a., 2011. Metabolic flux analysis of CHO cell metabolism in the late non-growth phase. Biotechnol. Bioeng. 108 (1), 82–92 (Jan).
Sheikh, K., Fo, J., Nielsen, L.K., 2005. Modeling hybridoma cell metabolism using a generic genome-scale metabolic model of Mus musculus,. Biotechnol. Prog. 21 (1), 112–121.
Simpson, N.H., Singh, R.P., Perani, a., Goldenzon, C., Al-Rubeai, M., 1998. In hybridoma cultures, deprivation of any single amino acid leads to apoptotic death, which is suppressed by the expression of the bcl-2 gene. Biotechnol. Bioeng. 59 (1), 90–98 (Jul).
Simpson, N.H., Singh, R.P., Emery, a.N., Al-Rubeai, M., 1999. Bcl-2 over-expression reduces growth rate and prolongs G1 phase in continuous chemostat cultures of hybridoma cells. Biotechnol. Bioeng. 64 (2), 174–186 (Jul.).
Smoot, M.E., Ono, K., Ruscheinski, J., Wang, P.-L., Ideker, T., 2011. Cytoscape 2.8: new features for data integration and network visualization. Bioinformatics 27 (3), 431–432 (Feb.).
Tait, S.W.G., Green, D.R., 2010. Mitochondria and cell death: outer membrane permeabilization and beyond. Nat. Rev. Mol. Cell Biol. 11 (9), 621–632 (Sep).
Templeton, N., Dean, J., Reddy, P., Young, J.D., 2013. Peak antibody production is associated with increased oxidative metabolism in an industrially relevant fed-batch CHO cell culture. Biotechnol. Bioeng. 110 (7), 2013–2024 (Feb).
Tey, B.T., Singh, R.P., Piredda, L., Piacentini, M., Al-Rubeai, M., 2000. Influence of bcl-2 on cell death during the cultivation of a Chinese hamster ovary cell line expressing a chimeric antibody. Biotechnol. Bioeng. 68 (1), 31–43 (Apr.).
Vance, J., 1990. Phospholipid synthesis in a membrane fraction associated with mitochondria. J. Biol. Chem. 265, 7248–7256.
Vaux, D., Cory, S., Adams, J., 1988. Bcl-2 gene promotes haemopoietic cell survival and cooperates with c-myc to immortalize pre-B cells. Nature 335 (29), 440–442.
Wei, Y., Pattingre, S., Sinha, S., Bassik, M., Levine, B., 2008. JNK1-mediated phosphorylation of Bcl-2 regulates starvation-induced autophagy. Mol. Cell 30 (6), 678–688 (Jul.).
Xie, L., Wang, D.I., 1996. Material balance studies on animal cell metabolism using a stoichiometrically based reaction network. Biotechnol. Bioeng. 52 (5), 579–590 (Dec.).
Xu, X., Nagarajan, H., Lewis, N.E., Pan, S., Cai, Z., Liu, X., Chen, W., Xie, M., Wang, W., Hammond, S., Andersen, M.R., Neff, N., Passarelli, B., Koh, W., Fan, H.C., Wang, J., Gui, Y., Lee, K.H., Betenbaugh, M.J., Quake, S.R., Famili, I., Palsson, B.O., Wang, J., 2011. The genomic sequence of the Chinese hamster ovary (CHO)-K1 cell line. Nat. Biotechnol. 29 (8), 1–8 (Jul.).
Youle, R.J., Strasser, A., 2008. The BCL-2 protein family: opposing activities that mediate cell death. Nat. Rev. Mol. Cell Biol. 9 (1), 47–59 (Jan.).
Young, J.D., 2013. Metabolic flux rewiring in mammalian cell cultures. Curr. Opin. Biotechnol., 1–8 (May).
Young, J.D., 2014. INCA: a computational platform for isotopically non-stationary metabolic flux analysis. Bioinformatics 30 (9), 1333–1335 (May).
Young, J.D., Walther, J.L., Antoniewicz, M.R., Yoo, H., 2008. An Elementary Metabolite Unit (EMU) based method of isotopically nonstationary flux analysis. Biotechnology 99 (3), 686–699.
Zagari, F., Stettler, M., Broly, H., Wurm, M., Jordan, M., 2013a. High expression of the aspartate–glutamate carrier Aralar1 favors lactate consumption in CHO cell culture. Pharm. Bioprocess. 1 (1), 19–27.
Zagari, F., Jordan, M., Stettler, M., Broly, H., Wurm, F.M., 2013b. Lactate metabolism shift in CHO cell culture: the role of mitochondrial oxidative activity. New Biotechnol. 30 (2), 238–245 (Jun.).
Zhang, J., 2010. Mammalian cell culture for biopharmaceutical production. 3rd ed. In: Baltz, R.H., Demain, A.L., Davies, J.E. (Eds.), Manual of Industrial Microbiology and Biotechnology, 104. ASM Press, Washington, DC, pp. 157–178.